



## Experiments on Gravel-Sand Transitions: Examination of Washload Deposition

Elizabeth H. Dingle<sup>1,2</sup>  and Jeremy G. Venditti<sup>3</sup> 

<sup>1</sup>Department of Geography, Simon Fraser University, Burnaby, BC, Canada, <sup>2</sup>Department of Geography, Durham University, Durham, UK, <sup>3</sup>School of Environmental Science, Simon Fraser University, Burnaby, BC, Canada

### Key Points:

- We generated a stable gravel-sand transition feeding sand onto a gravel bed in a narrow flume
- Sand was transported as washload through the gravel reach where the bed was at the threshold for entrainment, but as suspended bed material load in the sand reach
- Sand transitioned from washload to suspended bed material load at shear velocities of  $\sim 0.1$  m/s, consistent with the washload deposition theory

### Correspondence to:

E. H. Dingle,  
[elizabeth.dingle@durham.ac.uk](mailto:elizabeth.dingle@durham.ac.uk)

### Citation:

Dingle, E. H., & Venditti, J. G. (2023). Experiments on gravel-sand transitions: Examination of washload deposition. *Journal of Geophysical Research: Earth Surface*, 128, e2023JF007116. <https://doi.org/10.1029/2023JF007116>

Received 20 FEB 2023

Accepted 5 JUL 2023

### Author Contributions:

**Conceptualization:** Elizabeth H. Dingle, Jeremy G. Venditti  
**Data curation:** Elizabeth H. Dingle  
**Formal analysis:** Elizabeth H. Dingle  
**Funding acquisition:** Jeremy G. Venditti  
**Methodology:** Elizabeth H. Dingle  
**Supervision:** Jeremy G. Venditti  
**Visualization:** Elizabeth H. Dingle  
**Writing – original draft:** Elizabeth H. Dingle  
**Writing – review & editing:** Elizabeth H. Dingle, Jeremy G. Venditti

**Abstract** An abrupt transition in bed grain size occurs in river systems. Over a short downstream distance, often only a few channel widths, the bed surface fines from gravel ( $\sim 10$  mm) to sand ( $\sim 1$  mm). This is the gravel-sand transition (GST), and it is the only abrupt downstream reduction in grain size within fluvial systems. There are several theories for the origin of the GST, including size-selective deposition of bimodal grain size distributions and the rapid onset of washload deposition due to changes in particle suspension properties at shear velocities of  $\sim 0.1$  m/s. Here, we present a laboratory experiment examining changes in fluid and sediment dynamics across a GST. We developed a stable gravel bed reach that was just below the threshold of motion, then fed sand. We observed sand carried as washload in the gravel reach fall out of suspension, forming a sand bed and a stable GST. Shear velocity was  $0.09\text{--}0.10$  m/s upstream of the GST and  $<0.10$  m/s downstream, consistent with the washload deposition hypothesis. We were then able to perturb the position of the GST by systematically varying discharge and/or sand supply, shifting it downstream with an increase in discharge or a reduction in sediment supply. A decrease in discharge or increase in sand supply caused upstream migration. Our observations support an abrupt change in washload transport conditions across a narrow range of shear velocities, consistent with the washload deposition theory and measurements taken across GSTs in natural river systems.

**Plain Language Summary** The size of sediment on river bed surfaces typically fines gradually downstream. However, when gravel beds fine to a median grain size of  $\sim 10$  mm (fine gravel), an abrupt reduction in grain size occurs. Over a distance equivalent to a few channel widths, the characteristic grain size reduces to  $\sim 1$  mm (sand). This is the gravel-sand transition (GST). Several theories exist for why this abrupt grain size change occurs, and why it is specific to gravel and sand. Observations in rivers suggest that gravel-sand transitions occur where sediment is deposited from washload (sediment that is not persistently deposited in a reach) to suspended bed material load (sediment in suspension that is sourced from the bed). We undertook an experiment to see if a stable GST could be produced by washload deposition. We found that washload deposition can form a GST and that the transition will migrate by changing the sand supply and water discharge. Our experiments show that seasonal variations in sand supply and discharge drive short-term variability in the position of the transition.

## 1. Introduction

As gravel riverbed sediments gradually fine downstream, there is an abrupt reduction in median bed grain size that occurs at  $\sim 10$  mm. Over a distance as little as a couple of channel widths, river beds rapidly fine to  $\sim 1$  mm sand (Dingle et al., 2017, 2021; Ferguson et al., 1996; Frings, 2011; Kodama, 1994; Sambrook Smith & Ferguson, 1995; Shaw & Kellerhals, 1982; Venditti & Church, 2014; Yatsu, 1955). There is also a concurrent change from framework-supported gravel, to a matrix-supported sand bed structure (Frings, 2011; Venditti & Church, 2014). This is the gravel-sand transition (GST), and it is the only abrupt downstream reduction in median grain size in river bed sediments (e.g., Cui & Parker, 1998; Dingle et al., 2021; Ferguson et al., 1996; Parker & Cui, 1998; Sambrook Smith & Ferguson, 1995). A related phenomenon is the general paucity of river bed sediments with median grain sizes of  $\sim 1\text{--}5$  mm, more generally referred to as the grain size gap (e.g., Lamb & Venditti, 2016; Shaw & Kellerhals, 1982).

Two types of GSTs have been documented based on global analyses: those that occur through gravel exhaustion (e.g., in depositional basins downstream of mountain ranges) and those that appear to be forced by backwater-limits (Dingle et al., 2021). Gravel exhaustion GSTs form where gravel supply downstream of a moun-

© 2023 The Authors.

This is an open access article under the terms of the [Creative Commons Attribution-NonCommercial License](https://creativecommons.org/licenses/by-nc/4.0/), which permits use, distribution and reproduction in any medium, provided the original work is properly cited and is not used for commercial purposes.

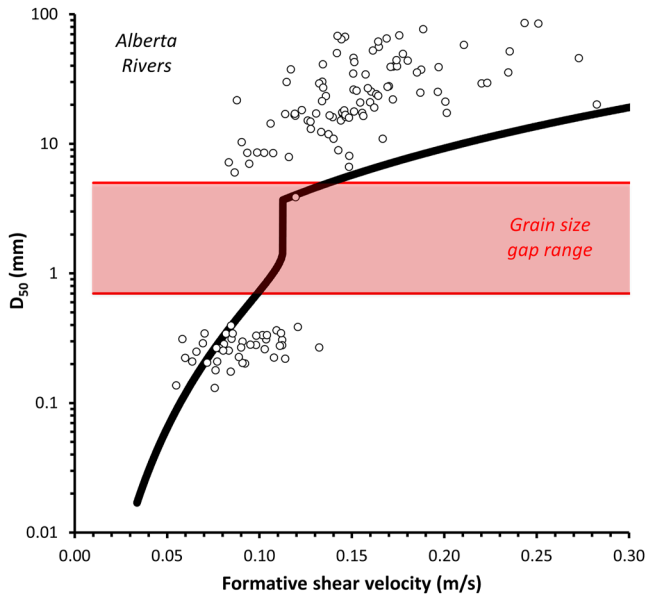


**Figure 1.** Predicted median grain size ( $D_{50}$ ) at the threshold of motion (black line) against formative (bankfull) shear velocity based on the theory developed by Lamb and Venditti (2016). Observations of the bed  $D_{50}$  for a series of rivers in Alberta (Canada) are also plotted with open circles.

tain range decreases through selective deposition, where deposition of the coarsest fraction is promoted through the generation of accommodation (e.g., subsidence, consolidation of sediment). Once gravel is exhausted from the supply, a break in water surface slope develops as sand bed rivers require lesser gradient to transport the incoming sand supply than gravel bed rivers (e.g., Ferguson, 2021; Lane, 1954; Parker et al., 2007). Other GSTs have been found to coincide with backwater limits upstream of local base level controls where a rapid decline in transport capacity of the river exists (e.g., Frings, 2011; Sambrook Smith & Ferguson, 1995). This may be coincidental, however, as the backwater limit may also form where gravel is exhausted from the system. While lower gradient sand reaches allow backwater reaches to extend considerable distances upstream, the steeper gravel gradient limits this extent (Dingle et al., 2021).

Early work on GSTs suggested that they formed by enhanced abrasion of fine gravel (Kodama, 1994; Yatsu, 1955), but the necessary attrition rates to produce an abrupt grain size change do not occur naturally (Attal & Lavé, 2009). Wolcott (1988) suggested that the bimodality of grain size distributions is linked to bedrock weathering that produces different modes, which may locally contribute to the abruptness of GSTs. The most prevalent proposed mechanisms for the emergence of GSTs are the size-selective transport of bimodal sediment mixtures. Field observations (Ferguson et al., 1996, 1998), laboratory experiments (Paola, Heller, & Angevine, 1992; Paola, Parker, et al., 1992; Seal et al., 1997; Toro-Escobar et al., 2000; Wilcock, 1998; Wilcock & Kenworthy, 2002) and numerical modeling using

bimodal and binary grain size distributions (Blom et al., 2017; Cui & Parker, 1998; Ferguson, 2003; Parker & Cui, 1998) suggest that GSTs emerge due to bedload sorting and a collapse of the ability of the flow to transport the sand mode as the gravel mode of a bimodal grainsize distribution distrains (Ferguson, 2003). The theory requires a bimodal bedload grain size distribution and does not recognize the role that suspension may play.

It has also been suggested that GSTs occur due to the rapid onset of washload deposition as gravel distrains from the bedload (Lamb & Venditti, 2016; Venditti & Church, 2014; Venditti et al., 2015, 2019). Direct measurements of sand transport in gravel and sand bed reaches of the Fraser River (British Columbia) document a shift in sand transport mode, from washload to suspended bed material load, across the GST (e.g., Venditti & Church, 2014; Venditti et al., 2015). In an alluvial river, the sediment load is comprised of bed material load and washload. Bed material load may be intermittently suspended or transported as bedload and should be well represented in lower bed and bank material (Church, 2006). In contrast, washload particles once entrained are not typically redeposited (e.g., Church, 2006; Colby, 1963; Garcia, 2008) and have advection lengths that greatly exceed the length of the reach (Venditti et al., 2015). Washload particles exchange with the bed but do not form persistent deposits, meaning that they are poorly represented in bed surface and bank grain size distributions (e.g., Lamb et al., 2020) and play minimal role in setting channel slope or width (e.g., Paola, 2001).

Lamb and Venditti (2016) showed that rivers dramatically lose the ability to transport sand as washload when the bed shear velocity ( $u^*$ ) falls below 0.1 m/s. They explored what happens to washload as the coarsest particles in the bedload mixture distrain and found a coincident change in the suspension threshold that results in washload deposition. They found that when the ninetieth percentile ( $D_{90}$ ) of a sediment mixture begins to deposit, the finest particles ( $D_{10}$ ) transition from being transported as washload to suspended bed material load. The shape of the bedload and suspension threshold curves lead to a dramatic change in the behavior of the median grainsize,  $D_{50}$ , at a formative flow with  $u^* = 0.1$  m/s (Figure 1), leading to a narrow range of conditions over which fine gravel beds can exist. At  $u^* > 0.1$  m/s, the  $D_{90}$  of the gravel bed is entrained and sand is carried as washload. At  $u^* < 0.1$  m/s, the  $D_{90}$  grain size is deposited and sand that had been carried as washload transitions to suspended bed material load, forming the sand bed. Observations of shear velocity across the GST support the prediction (Figure 1). The washload theory is powerful in that it predicts the formation of GSTs without imposing a bimodal grain size distribution and provides an explanation for the paucity of rivers with median bed grain sizes of  $\sim 1$ –5 mm. Support for the washload theory lies in field observations of transport modes of sand (Venditti & Church, 2014;

Venditti et al., 2015, 2019) and a meta data analysis of flow and grain size across GSTs (Lamb & Venditti, 2016). Experiments designed to isolate the washload deposition mechanism are needed.

Here, we present a phenomenological flume experiment to test the hypothesis that a stable and abrupt GST can be formed by washload deposition alone, without the contingencies that exist in the field. The alternative outcome is that we cannot produce a stable or abrupt GST by washload deposition, and instead produce an unstable mixed gravel and sand bed with a poorly defined transition, where sand is carried as suspended bed material load through the length of the flume. We then explore how sand is transported across and deposited downstream of the stable GST in response to a range of perturbations in discharge and sediment supply. In a companion paper, we examine the behavior of grain size gap material and how washload deposition affects gap material at the GST. In this paper, the objectives of our experiment were to (a) explore whether it is possible to generate a stable gravel bed with sand transported as washload, (b) observe how a sand bed develops downstream of a gravel reach, (c) document the shear velocities across stable GSTs, and (d) document how stable GSTs respond to changes in discharge and sand supply.

## 2. Methods

### 2.1. Prototype and Design

We elected to examine gravel exhaustion GSTs as their emergence is governed by sediment dynamics; however, we also imposed backwater effects on stable gravel exhaustion GSTs in one run by increasing the flume base-level. Previous flume experiments have examined size selective sorting of bed sediment using bimodal sediments (e.g., Curran & Wilcock, 2005; Paola, Heller, & Angevine, 1992; Paola, Parker, et al., 1992; Sambrook Smith & Ferguson, 1996; Wilcock & Kenworthy, 2002; Wilcock et al., 2001), but experiments designed to produce GSTs by size-selective transport have required use of extremely long flumes for the process to occur (e.g., Paola, Heller, & Angevine, 1992; Paola, Parker, et al., 1992; Seal et al., 1997; Toro-Escobar et al., 2000; Wilcock, 1998) making experimental investigations impractical. Here, we take advantage of the “unreasonable effectiveness” approach to geomorphology experimentation (Paola et al., 2009), where we undertake a phenomenological experiment, where we only scale parameters that we expect control the process of interest. In doing so, we are testing whether a particular set of variables is capable of producing a phenomenon.

In our experiment, we build a stable GST that is temporally and spatially fixed, where gravel is just below the threshold for entrainment, and only sand is fed into the flume. Our approach is based on observations of natural systems, where there may only be a few days or weeks per year when significant gravel transport across the GST would be expected to occur (i.e., during high flow conditions). In contrast, sand is continuously transported in gravel bed and sand bed reaches (e.g., Church et al., 1991; Kuhnle, 1993; Wathen et al., 1995; Wilcock, 1998). This phenomenological experiment is not designed to replicate or serve as a scaled model of natural river channels, but instead to study a core process that may be responsible for GST formation. As such, care must be taken in extrapolating from our unscaled, phenomenological experiment to natural systems.

Through their global analysis, Dingle et al. (2021) established that the only universal morphological characteristic observed in GSTs is the abrupt reduction in grain size from 5 to 10 mm gravel to sand. Given that the phenomenon is specific to these grain sizes, we elected not to scale grain size in our experiment, but instead retained these sizes and scaled the flow to produce specific transport stages of gravel and sand that are linked to their entrainment and suspension thresholds.

### 2.2. Experimental Setup

The experiment was conducted in a 5-m long, 34-mm wide flume (Figure 2). In many field examples, a diffuse extension of the GST also exists, which can persist for tens of channel widths equivalent (Venditti & Church, 2014; Venditti et al., 2015). Our flume was much longer than it was wide to ensure that sand and gravel reaches were greater in length than the predicted diffuse extension. The width allowed the coarsest grain sizes to pass one another laterally, without jamming and eliminated cross-stream transport, lateral sorting and bar formation. Use of a small flume also increases the number of experimental runs we can do because of faster run times (e.g., Dudill et al., 2017, 2020; Frey, 2014; Frey et al., 2020; Hergault et al., 2010).

We built a gravel reach that extended halfway down the flume, then added a sand feed to the gravel reach. Water was recirculated using a pump to ensure a constant discharge throughout each run, but sediment was not

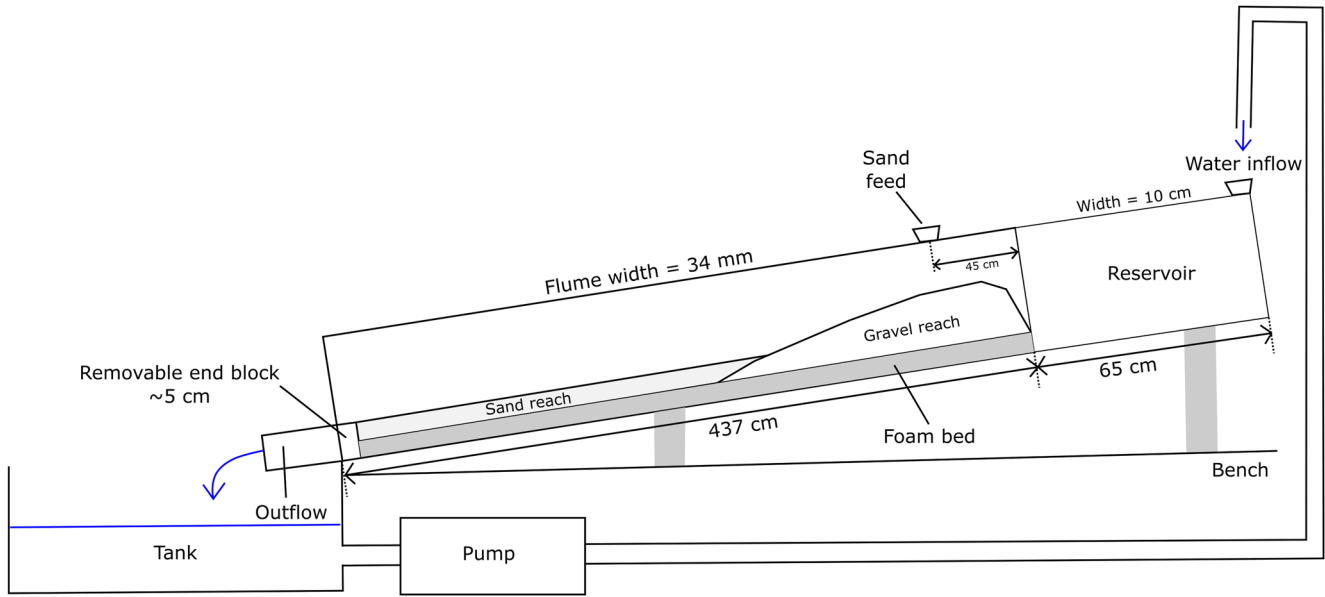


Figure 2. Narrow flume (not to scale).

recirculated. A 5 cm high block was inserted at the end of the flume to prevent all sediment from washing out and acted as base level for the experiment. Sand was fed at a constant rate into the flume using a sediment hopper at the top end of the flume (Figure 2).

Our gravel reach was composed of a unimodal gravel with a  $D_{50} = 9.8$  mm and the sand feed was a unimodal sand with  $D_{50} = 0.57$  mm (Figure 3). Flow conditions were established in the gravel section so that the Shields number ( $\tau_*$ ) was just below the threshold for motion. The Shields number is defined as follows:

$$\tau_* = \frac{\tau_b}{(\rho_s - \rho_w)gD} \quad (1)$$

where  $\tau_b$  is the shear stress at the bed,  $D$  is the diameter of a particle and is usually taken as the bed surface  $D_{50}$ ,  $\rho_s$  and  $\rho_w$  are the densities of the sediment and fluid, respectively, and  $g$  is gravitational acceleration. Values of  $\tau_* < 0.045$  are widely accepted as characterizing conditions below the entrainment threshold for a gravel mixture (Miller et al., 1977; Yalin & Karahan, 1979). The flow was also established such that shear velocity  $u^* = \sqrt{(\tau_b/\rho)}$  exceeded the settling velocity of the sand by  $\sim 3$  times, which is widely thought to produce washload conditions (Lamb & Venditti, 2016, and references therein). We tested these threshold conditions in our experiments to ensure the flow was producing the transport stages anticipated to produce the GST and tweaked the flow conditions as necessary.

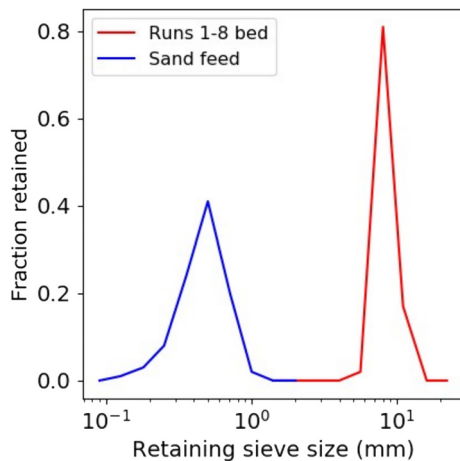


Figure 3. Grain size distributions of the gravel bed (red) and sand feed (blue).

### 2.3. Experimental Procedure and Observations

Our experiment focused on the formation of a stable GST and responses to perturbations in water discharge ( $Q$ ) and sand supply ( $Q_s$ ). In each run, we deposited the 9.8 mm gravel and turned on the flow to build the gravel bed with a gradient where the sediment was at the threshold for motion. We then turned on the sand feed, which formed a stable gravel exhaustion GST (Run 1). We then examined how the position of the GST responded to: (a) base level change of the system (Run 2), (b) increases and decreases in  $Q$  and  $Q_s$  separately (Runs 3–6), and (c) changes in  $Q$  and  $Q_s$  together (Runs 7–8; Table 1). The backwater was produced by increasing the height of a gate at the end of the flume from 5 to 12 cm, which increased the downstream water level and generated a transient backwater profile that ended half-way

**Table 1**  
*Run Numbering and General Description*

Run ID	Run description
Run 1	Stable GST, sand feed only
Run 2	Perturbed GST, change in base level
Run 3	Perturbed GST, increase $Q$
Run 4	Perturbed GST, decrease $Q$
Run 5	Perturbed GST, increase $Q_s$
Run 6	Perturbed GST, decrease $Q_s$
Run 7	Perturbed GST, increase $Q$ and $Q_s$
Run 8	Perturbed GST, decrease $Q$ and $Q_s$

a laser Doppler velocimeter operated at an effective frequency of 50 Hz. Three sets of vertical profiles were measured with a vertical resolution of 2 mm within the gravel bed reach, the diffuse GST reach, and the sand bed reach to obtain local shear stresses (9 profiles in total). Sand coverage could not be measured accurately during runs because it was difficult to distinguish sand from gravel through water (see Figure 4), and when the flow was stopped, sand was deposited on the bed, making it appear as though the sand coverage was greater than it was with flow. We therefore estimated sand coverage as  $\sim 15\%$  in the gravel reach (Figure 4a), which is a typical value for the volumetric content of sand in clean gravel bed rivers where sand only fills interstitial spaces (e.g., McLean, 1990; Shaw & Kellerhals, 1982). This may overestimate the sand coverage because the surface distribution of sand is typically less than the volumetric content (e.g., Graham et al., 2005). It was not possible to measure washload and suspended bed material load directly as our runs evolved quickly and physical measurements with siphons or bedload traps would have radically altered the small-scale experiments; therefore, we rely on direct visual observations to characterize the transport modes and support them with calculations of well-established suspension criteria.

#### 2.4. Data Analysis

At-a-point velocity data were time-averaged, then spatially averaged to produce double-averaged velocity profiles (Nikora et al., 2001), from which we calculated local shear velocity ( $u^*$ ) from the law of the wall by plotting double-averaged velocity ( $U_m$ ) as a function of height above the bed ( $z$ ). Local shear velocity was calculated as  $u^* = \kappa a$  where  $\kappa$  is the von Karman constant (0.41) and  $a$  is the slope of a least squares regression between  $U_m$  and  $\ln(z)$ . Reach-averaged shear velocity ( $u_r^*$ ) for both the gravel and sand reaches was also calculated from a reach-averaged shear stress ( $\tau$ ) where:

$$u_r^* = \sqrt{\frac{\tau}{\rho}} = \sqrt{ghS} \quad (2)$$

where  $\rho$  is the density of water,  $g$  is the acceleration due to gravity,  $h$  is the flow depth and  $S$  is the water surface slope. Reliably calculating  $\tau$  using this reach-averaged method is challenging in a narrow channel because a portion of the total force is applied to the sidewalls and therefore not available to transport sediment. We therefore elected to apply a sidewall correction to the data as originally proposed by Williams (1970); however, we treat this calculation of corrected  $\tau$  as an index of the true shear stress. Substituting depth and a sidewall correction for the hydraulic radius in Equation 2, resulted in  $<6\%$  difference in  $u_r^*$  values.

We calculated the reach-averaged velocity as  $\bar{U} = Q/(hw)$ , where  $w$  is flume width, in both the sand and gravel reaches. Particle Reynolds number ( $R_p$ ) was also calculated for both the gravel and sand reach in each run:

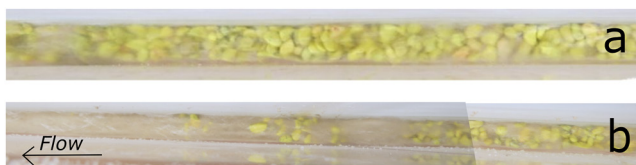


**Figure 4.** (a) Stable gravel-sand transition (GST) gravel bed surface showing a small fraction of sand present on the surface, (b) photo of diffuse GST extension downstream of the gravel reach.

up the gravel wedge. Each run ended when gravel particles were immobile, the longitudinal profile was static, and the position of the GST remained stationary for at least 5 min.

Discharge measurements were taken once the flume was in an equilibrium state with a fully developed GST. Measurements of flow depth ( $h$ ), and bed and water surface gradients ( $S$ ) were made for each initial condition, and at the end of the run after the perturbation by changes in  $Q$  or  $Q_s$ . We also measured the position of the GST where the first persistent patches of sand covering gravel were observed on the bed. The new stable GST position following each perturbation was similarly recorded when the gravel reach had been stable (i.e., particles were immobile) for at least 5 min, and the sand feed was passing directly through the flume (i.e., interstitial spaces in the gravel reach were filled with sand).

In Runs 1 and 2, we also measured velocity profiles when the GST was stable (after the base level perturbation in Run 2). Profiles were measured using

$$R_p = \frac{D_{50} \sqrt{Rg D_{50}}}{\nu} \quad (3)$$

where  $\nu$  is the kinematic viscosity of water, and  $R$  is submerged specific gravity incorporating the density of sediment ( $\rho_s$ ) where  $R = (\rho_s/\rho) - 1$  (Garcia, 2008). Particle settling velocities ( $\omega$ ) were calculated using the Ferguson and Church (2004) formula to calculate a suspension ratio ( $u^*/\omega$ ) to characterize sand transport mode to compare with our visual observations. Incipient bed material suspension occurs when  $u^*/\omega > 0.4$  when the flow is hydraulically rough ( $R_p > 27.5$ ). At  $R_p < 27.5$ , the threshold for suspension is a function of  $R_p$  (Nino et al., 1994; Niño et al., 2003). The transition to washload is typically assumed to occur at three times the suspension threshold ( $u^*/\omega = 1.2$ ) (Bridge, 2009), although this boundary has yet to be precisely defined through rigorous experiments. An advection length ( $A_L$ ) for sand being fed into the flume was also calculated as follows:

$$A_L = \bar{u}h/\omega \quad (4)$$

where  $\bar{u}$  is the mean flow velocity within the entire gravel reach. Venditti et al. (2015) showed that when  $A_L \approx$  channel width, particles move as suspended bed material, but when  $A_L \gg$  channel width, particles are moved as washload.

### 3. Results

#### 3.1. Flow and Shear Stress

Locally derived  $u^*$  values from velocity profiles in Runs 1 and 2 show a reduction from 0.1 m/s in the gravel reach to 0.07–0.08 m/s in the sand reach (Figure 5). Measurements from within the diffuse GST were 0.08 and 0.10 m/s in Runs 1 and 2, respectively. Reach-averaged  $u^*$  measurements obtained using the depth-slope product show a similar reduction across the GST, although measurements within the sand reach are notably lower than the laser-derived measurements, at 0.04–0.05 m/s (Table 2; Figure 6). Nevertheless, both methods suggest a reduction in shear velocity across the GST at values of 0.08–0.10 m/s (Figure 6), which is consistent with both theoretical predictions and field observations (Lamb & Venditti, 2016).

In all runs, the Froude number was transcritical to supercritical in both the gravel and sand reaches with values between 1.0 and 1.5 (Table 2). Flow depths were similar in the gravel and sand bed reaches and there were no hydraulic jumps observed. The flow feature across the GSTs was similar to a backwater, but the flow was supercritical, suggesting that flow in the sand bed reach was primarily responding to changes in base level, which produce an effect that is similar to imposing a backwater. Transient standing waves did occur in some experiments but did not affect scour and fill patterns in the flume. The phenomena we explore are not affected by the flow being transcritical or supercritical because lift and drag forces applied to a particle are caused by the distribution of velocity around the particle, which is not related to the Froude number.

#### 3.2. Formation of a Stable Gravel-Exhaustion GST (Run 1)

We were able to generate a stable GST by feeding sand onto an otherwise immobile gravel wedge, where the gravel was at the threshold of motion (Figure 7a). When the sand feed was turned on, sand passed through the gravel reach as washload (in suspension without interacting with the bed), although some sand was interstitially trapped as sediment laden water flow passed through the bed, as is typical in gravel bedded rivers (e.g., Church, 2006; Frings, 2008). This exchange of washload sediment without forming persistent deposits is typical of washload (Einstein, 1968; Lamb et al., 2020). The Shields number ( $\tau^*$ ) for the gravel wedge and our flow conditions varied between 0.047 and 0.071, depending on the run (Table 2), which is just above the widely accepted threshold of motion for gravel mixtures of 0.045 (e.g., Miller et al., 1977; Yalin & Karahan, 1979), but comparable to values of 0.065–0.117 obtained in flume experiments with structured gravel beds (Church & Hassan, 2005; Hassan et al., 2020). This confirms that our gravel wedge was at or near the threshold of motion. As flow spilled over the block at the end of the flume, a short (~5–10 cm) drawdown profile developed but had no influence on sediment movement upstream. The GST was generally a 20–40 cm region of patchy gravel and sand (Figure 4b), similar to the diffuse extension observed in many GSTs (cf., Venditti & Church, 2014; Venditti et al., 2015). For sand in the gravel reach,  $A_L = \sim 20$  cm, whereas the GST occurred  $> 50$  cm downstream of the sediment feeder, suggesting that sand had opportunity to actively exchange with the bed in the gravel-reach, even though persistent deposits did not form.

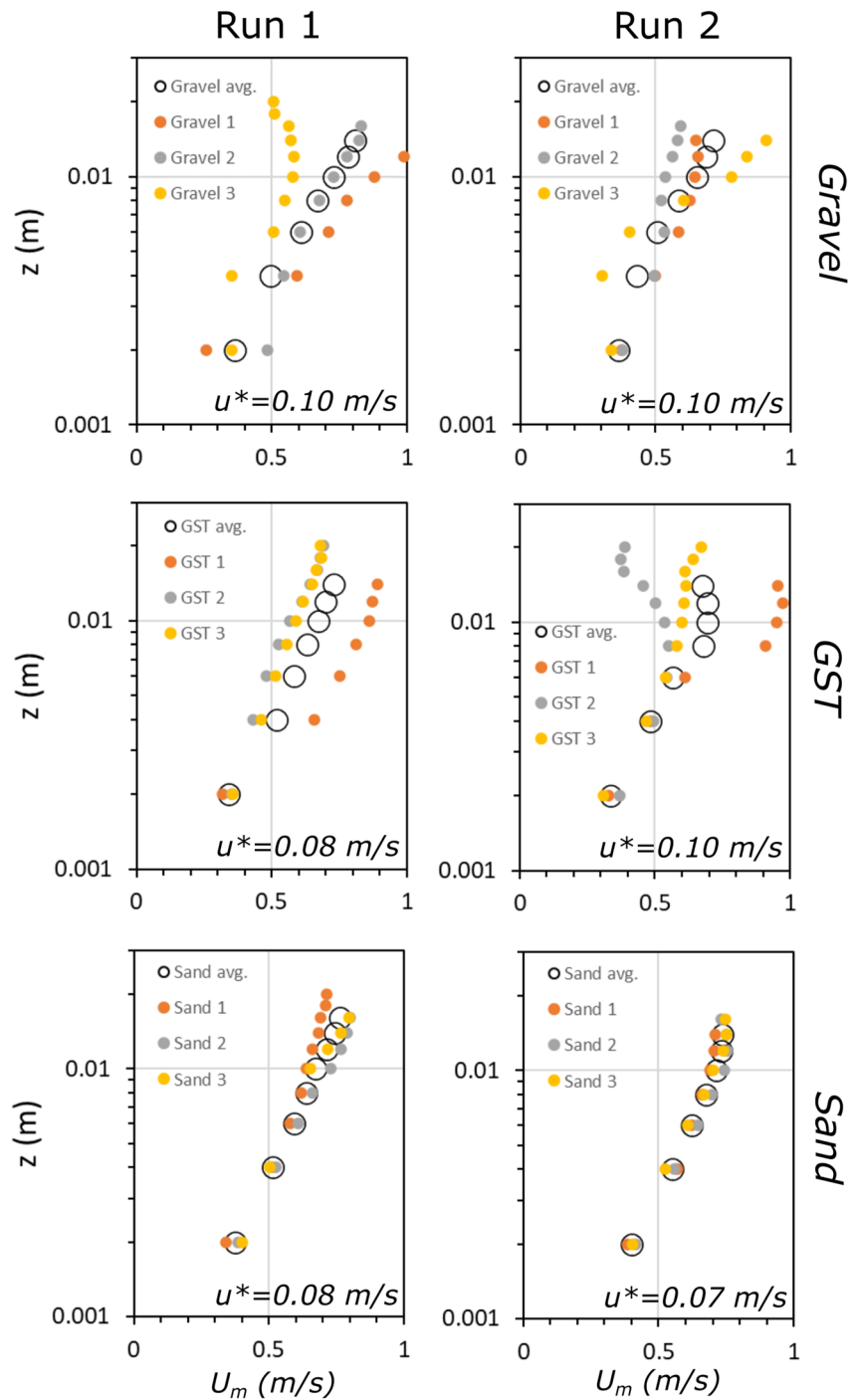


**Figure 5.** Double averaged velocity ( $U_m$ ) against elevation above the bed ( $z$ ) and associated shear velocity ( $u^*$ ) for Runs 1 and 2.

Observations of sand transport in the gravel reach indicated that sand was transported as washload, interacting with the gravel bed but without forming persistent deposits. The suspension ratio  $u_r^*/\omega = 1.2$  in the gravel reach indicating washload transport. Downstream of the transition, sand was carried as suspended bed material load and  $u_r^*/\omega = 0.45$ , which is above the suspension threshold, but below the nominal washload threshold. The particle Reynolds number ( $Re_p$ ) reduced from 2074 in the gravel reach to 30 in the sand reach, indicating that the flow was hydraulically rough in both reaches, but just marginally so in the sand reach.

**Table 2**  
*Stable (and Perturbed) Gravel-Sand Transition Hydraulic Conditions in Gravel (g) and Sand (s) Reaches, and Sediment Feed Details for Runs 1–8*

Run ID	$Q$ (l/s) <sup>a</sup>	$S$ (-/-) <sup>a</sup>	$h$ (cm) <sup>a</sup>	$\bar{U}$ (m/s) <sup>a</sup>	$u^*$ , corrected (m/s)	$Re_p$	$u^*/\omega$	$A_L$ (cm)	Froude number	Initial gravel reach $r^*$	Sediment feed ( $D_{50}$ and feed rates, before and after perturbation where applicable)
1	0.557	0.080 (g)	2.25 (g)	0.73 (g)	0.09 (g)	2,074 (g)	1.18 (g)	21	1.5 (g)	0.055	Sand—0.57 mm (3.4 g/s)
		0.012 (s)	2.25 (s)	0.73 (s)	0.04 (s)	30 (s)	0.45 (s)		1.5 (s)		
2	0.553	0.068 (g)	2.00 (g)	0.78 (g)	0.08 (g)	2,074 (g)	1.06 (g)	20	1.8 (g)	0.044	Sand—0.57 mm (3.4 g/s)
		0.016 (s)	2.35 (s)	0.67 (s)	0.04 (s)	30 (s)	0.54 (s)		1.4 (s)		
3	0.497/0.652	0.093/0.083 (g)	2.75/3.00 (g)	0.53/0.64 (g)	0.10 (g)	1,786 (g)	1.30 (g)	18	1.0/1.2 (g)	0.071	Sand—0.57 mm (3.4 g/s)
		0.017/0.020 (s)	2.55/3.00 (s)	0.57/0.64 (g)	0.04 (s)	26 (s)	0.54 (s)		1.1/1.2 (s)		
4	0.601/0.270	0.092/0.095 (g)	2.85/1.75 (g)	0.62/0.45 (g)	0.10 (g)	1,786 (g)	1.30 (g)	22	1.2/1.1 (g)	0.071	Sand—0.57 mm (3.4 g/s)
		0.022/0.025 (s)	2.85/1.70 (s)	0.62/0.47 (s)	0.05 (s)	26 (s)	0.64 (s)		1.2/1.1 (s)		
5	0.556	0.102/0.131 (g)	2.85/2.80 (g)	0.57/0.58 (g)	0.11 (g)	2,074 (g)	1.41 (g)	21	1.1/1.1 (g)	0.079	Sand—0.57 mm (3.4 g/s) and 5.62 g/s
		0.020/0.023 (s)	2.75/2.65 (s)	0.59/0.62 (s)	0.05 (s)	30 (s)	0.62 (s)		1.1/1.2 (s)		
6	0.577	0.074/0.069 (g)	2.95/3.00 (g)	0.57/0.57 (g)	0.09 (g)	1,786 (g)	1.18 (g)	21	1.1/1.0 (g)	0.058	Sand—0.57 mm (3.4 g/s) and 1.96 g/s
		0.024/0.018 (s)	3.00/2.95 (s)	0.57/0.58 (s)	0.05 (s)	26 (s)	0.67 (s)		1.0/1.1 (s)		
7	0.612/0.753	0.072/0.077 (g)	2.85/3.40 (g)	0.64/0.65 (g)	0.09 (g)	1,786 (g)	1.15 (g)	23	1.2/1.1 (g)	0.056	Sand—0.57 mm (3.4 g/s) and 5.62 g/s
		0.021/0.023 (s)	3.00/3.30 (s)	0.61/0.67 (s)	0.05 (s)	26 (s)	0.62 (s)		1.1/1.2 (s)		
8	0.641/0.528	0.092/0.082 (g)	2.90/2.40 (g)	0.65/0.65 (g)	0.10 (g)	1,786 (g)	1.31 (g)	23	1.2/1.3 (g)	0.072	Sand—0.57 mm (3.4 g/s) and 1.96 g/s
		0.018/0.013 (s)	2.85/2.75 (s)	0.66/0.56 (s)	0.05 (s)	26 (s)	0.58 (s)		1.3/1.1 (s)		

<sup>a</sup>Initial and final (after perturbation) values are separated by /.

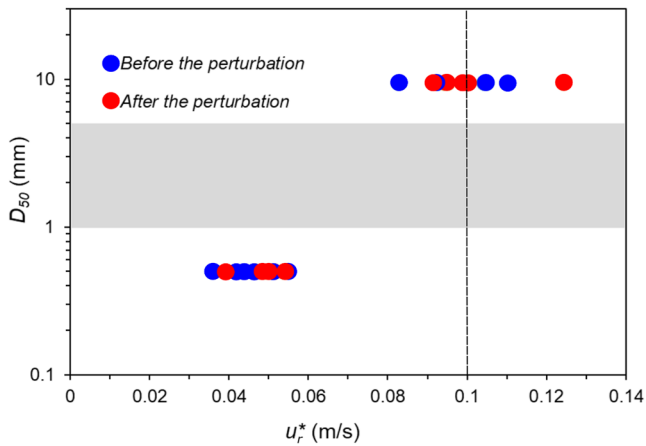


**Figure 6.** Median bed grain size and reach-averaged shear velocity ( $u_r^*$ ) before and after the perturbation in discharge and/or sand supply. The vertical dashed line represents the predicted threshold at which sand transitions from washload to suspended bed material load (Lamb & Venditti, 2016), and the gray box represents the grain size gap range.

### 3.3. Base Level Change Perturbation (Run 2)

Increasing the height of the end gate in the flume 5–12 cm increased the base level in our experiment. Initially, a backwater formed with a break in water slope approximately halfway down the initial gravel wedge. Based on a uniform sand bed channel, we would expect a transient backwater length of ~7 m to be generated by this increase in block height. However, because we have a pre-existing break in bed gradient caused by the GST, the transient backwater is much shorter (~2.75 m) as the gravel wedge is much steeper than the sand bed. The length of the transient backwater here is controlled both by the increase in base level and by the pre-existing break in bed slope and steeper gravel bed gradient. Sand then started to fall out of suspension at the position of this new break in water surface slope and aggraded the sand bed. As the accommodation space produced by the base level increase filled with sediment, the water levels responded passively and we were able to force the stable GST to migrate ~85 cm upstream (Figure 7b). The backwater then disappeared. Sand that had been carried as washload in the gravel reach started depositing immediately downstream of the break in water surface slope and the sand deposition mobilized some gravel in the lower portion of the gravel wedge due to the enhanced mobility of gravel with sand deposits on the surface (e.g., Curran & Wilcock, 2005; Wilcock, 1998; Wilcock & Crowe, 2003; Wilcock & Kenworthy, 2002). Sand continued to deposit downstream of the break in water surface slope until the sand bed aggraded

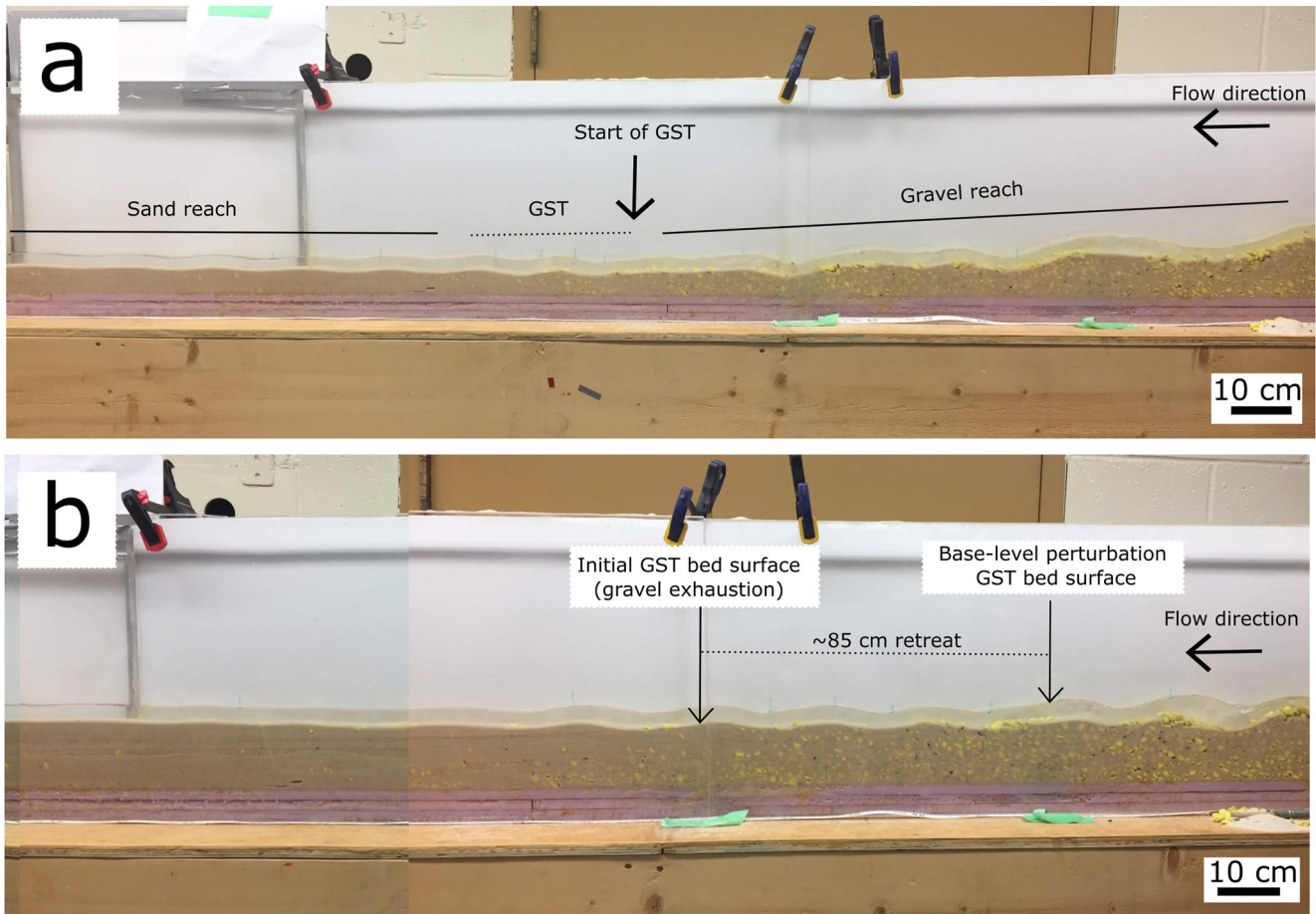


**Figure 7.** (a) Stable gravel-sand transition (GST) with a sand feed only (Run 1). (b) Base-level change mediated GST (Run 2).

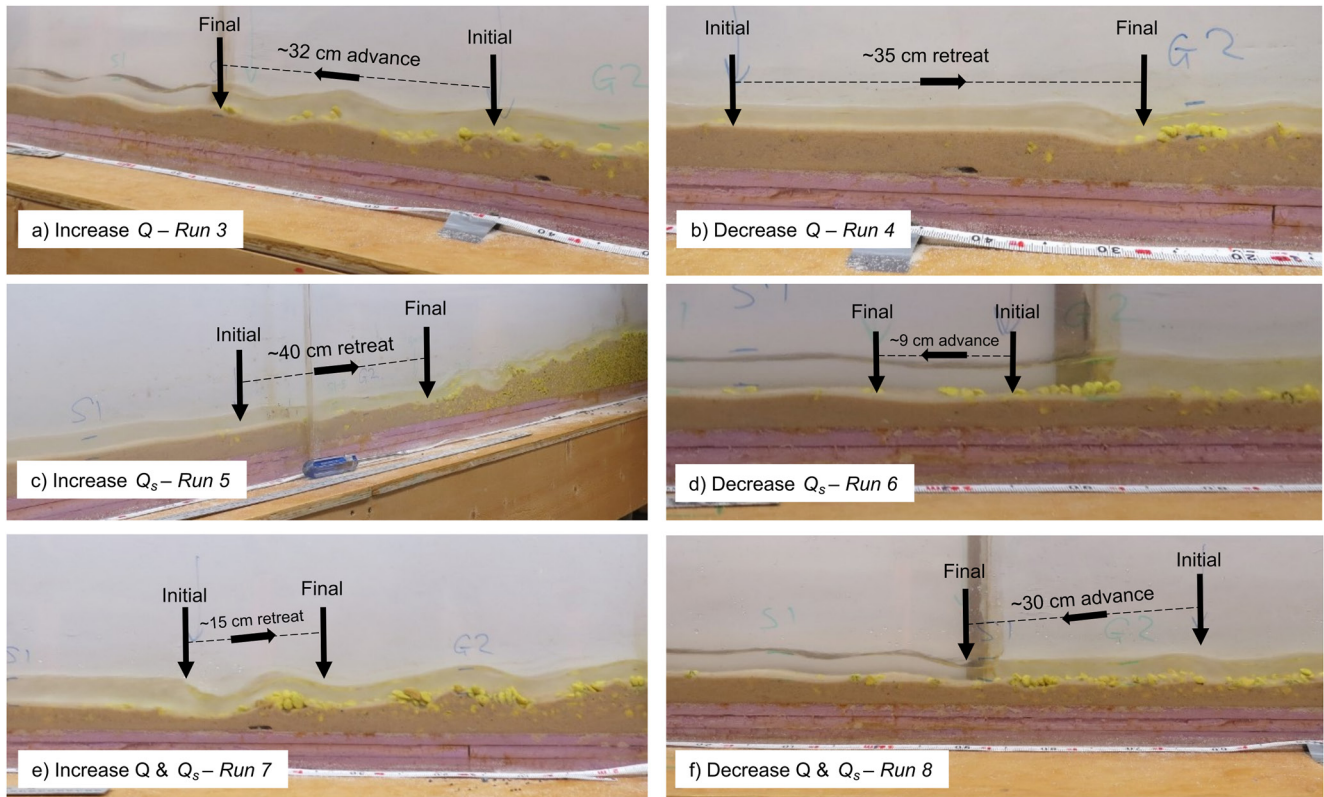


**Figure 8.** Changes in the position of the gravel-sand transition in response to an (a) increase in water discharge ( $Q$ ), (b) decrease in  $Q$ , (c) increase in sand supply ( $Q_s$ ), (d) decrease in  $Q_s$ , (e) increase in both  $Q$  and  $Q_s$ , (f) decrease in both  $Q$  and  $Q_s$ . Flow is right to left in each panel.

to the flume end gate elevation, and the backwater disappeared. Similar to the gravel-exhaustion case, sand passed through the gravel reach as washload and as suspended bed material load in the sand reach both during and after the perturbation. Across the perturbed GST,  $u_r^*/\omega$  reduced from 1.06 to 0.54 while  $u_r^*$  reduced from 0.08 to 0.04 m/s.

### 3.4. Perturbation of a Stable Gravel-Exhaustion GST (Runs 3–8)

Increasing water discharge ( $Q$ ) in Run 3 from 0.50 to 0.65 l/s resulted in a ~32 cm downstream migration of the GST within ~5 min (Figure 8a). Particles in the gravel reach were mobilized and transported across the GST where they settled on the bed, advancing the GST downstream. Sand was suspended through this extension of the gravel reach. Some gravel particles mobilized by the increase in  $Q$  also rafted through the sand reach and exited the flume. There was an overall reduction in the gravel reach gradient from 0.093 to 0.083. In the gravel reach,  $u_r^*$  remained at 0.10 m/s before and after the perturbation. Decreasing  $Q$  in Run 4 from 0.60 to 0.27 l/s resulted in a ~35 cm upstream retreat of the GST (Figure 8b), which was stable after ~10 min. Within the gravel reach,  $u_r^*$  reduced from 0.10 to 0.09 m/s, but remained unchanged in the sand reach. A patchy sand cover developed in the gravel bed because  $u_r^*/\omega$  fell below the washload threshold and sand was transported as suspended bed material load after the perturbation.

Increasing  $Q_s$  in Run 5 resulted in a ~40 cm retreat of the GST as sand started depositing at the upstream of the GST, burying underlying gravel (Figure 8c). There was a small increase in the gravel and sand reach water surface gradients. The GST was stable after ~15 min. Reducing  $Q_s$  while keeping  $Q$  constant in Run 6 resulted in a small downstream progradation of the GST (~10 cm). Rather than gravel being mobilized and deposited at the GST, reducing sand supply resulted in uncovering of the previously buried gravel immediately upstream of the GST, in the tapered gravel wedge (Figure 8d). There was a marginal increase in  $u_r^*$  from 0.11 to 0.12 m/s within the gravel reach, further increasing  $u_r^*/\omega$  from 1.41 to 1.59.

Increasing both  $Q$  and  $Q_s$  (Run 7) resulted in a  $\sim 15$  cm upstream retreat in the GST (Figure 8e), which stabilized after  $\sim 14$  min. The ratio of  $Q_s/Q$  (i.e., sediment concentration) increased from 6.4 to 7.5 g/l. The gravel reach became slightly sandier, with small sand patches developing on the bed representing an upstream migration of the GST. There was no change in  $u_r^*$  or  $u_r^*/\omega$  within the gravel reach. Decreasing both  $Q$  and  $Q_s$  in Run 8, where the ratio of  $Q_s/Q$  decreased from 6.2 to 3.7 g/l, resulted in a  $\sim 30$  cm advance of the GST (Figure 8f), which stabilized after  $\sim 5$  min. Like Run 6, downstream migration of the GST was driven by the uncovering of previously buried gravel particles, rather than mobilization of material from the gravel wedge. There was no change in  $u_r^*$  or  $u_r^*/\omega$  within the gravel reach.

In some runs, particularly during the transition between states after a perturbation and in the GST extension, we observed undulations in the bed (e.g., Figure 8), although these were often temporary. Clustering of the coarsest gravel particles locally strengthened small portions of the gravel bed (Church & Hassan, 2005; Hassan et al., 2020; Church et al., 1998), while adjacent areas were relatively weaker. This resulted in along stream variation in the bed strength and created an undulating surface with standing waves. This bed structuring accounts for the relatively high  $\tau^*$  values observed in the gravel reach.

## 4. Discussion

### 4.1. Implications for GSTs in Rivers

Our phenomenological experiment was designed to focus on the known common characteristics associated with GSTs, based on decades of field observations, so that we could explore sediment dynamics across the GST and after a discharge or sediment supply perturbation. The narrow flume was not intended as a scale model of a river; yet, by using grain sizes typical of those across a GST, we are able to reproduce the same reduction in  $u^*$  across the GST as observed in natural systems. Measurements of  $\tau^*$ ,  $Re_p$  and  $u_r^*/\omega$  were also consistent with those observed in natural river systems with the same bed grain sizes, implying that our experiment successfully captured key dynamics that control sediment entrainment and suspension across a GST. Additional work is needed to explore whether the same  $u^*$  values and GST abruptness can be reproduced with the wider gravel grain size distribution typical of rivers. Further experiments in a wider channel are also warranted to explore how lateral variation in sediment sorting and bar formation affect the emergence of GSTs by washload deposition.

### 4.2. Can the GST Be Formed by Washload Deposition?

Lamb and Venditti (2016) used theoretical reasoning to suggest that GSTs can form by suspension fallout because when 10 mm gravel begins to deposit from bedload, sand should transition from being transported as washload to suspended bed material load. The washload deposition theory further predicts that this should occur at a formative (or bankfull)  $u^* = 0.1$  m/s. Direct observations from rivers in western Canada (e.g., Lamb & Venditti, 2016; Venditti et al., 2015) support the prediction (Figure 1) as do the present experimental runs. Our calculations of  $u_r^*$  show there is a dramatic change in suspension dynamics across the GST. We observed sand passing through the gravel reach as washload (without forming persistent surface deposits) and the nominal washload threshold  $u_r^*/\omega = 1.2$  was exceeded. Near the toe of the gravel wedge, sand was observed to start settling on the bed, after which it was transported through the flume as suspended bed material load where  $u_r^*/\omega < 0.70$ . This change in suspension dynamics across the transition corresponds to threshold  $u^*$  values of  $\sim 0.1$  m/s.

### 4.3. Morphology and Migration of Gravel-Sand Transitions

The GST is typically abrupt with a framework supported gravel wedge deposit and a lower gradient sand deposit. Many GSTs have been documented to have a diffuse extension (e.g., Arb3s et al., 2021; Dingle et al., 2020; Venditti & Church, 2014; Venditti et al., 2015, 2019) where gravel leaks beyond the abrupt transition. Our experiments were designed to have a gravel wedge, but we also observed the experimental GSTs to have a diffuse extension. The length of the diffuse extension varies seasonally in many rivers. For example, there are seasonal changes in bed surface sand cover documented across the diffuse extension of the GST in the Fraser River that have been interpreted as downstream migration (Blom et al., 2017), even though the GST appears to have been in approximately the same location for millennia (Roberts & Morningstar, 1989). During low flow, seasonal cover sand develops at the end of the gravel reach but is washed downstream during periods of higher flow, re-exposing

the gravel bed (Venditti et al., 2015). Our experiment suggests that changes in discharge, sediment supply and the sediment delivery ratio can cause the GST to appear to migrate upstream or downstream in a similar fashion.

While the position of our experimental GST was effectively controlled by the amount of gravel that was initially deposited within the flume and the imposed discharge (gravel exhaustion), we were able to cause it to migrate by perturbing the water and sand supply (i.e., there was no gravel input). This migration appeared to occur through two mechanisms. First, increasing  $Q$  mobilized gravel particles, resulting in them over-running the initial GST position. In contrast, reducing  $Q_s$  also resulted in downstream migration of the GST, but through the uncovering of buried gravel particles downstream of the initial GST location (i.e., no gravel moved). Reducing  $Q$  or increasing  $Q_s$  resulted in an upstream migration of the GST due to the burial of gravel by sand. When maintaining the  $Q$  to  $Q_s$  ratio in Run 7, there was minimal change to the position of the GST. In Run 8, when the  $Q$  to  $Q_s$  ratio was decreased, the GST migrated downstream. Combined, these results suggest that the position of the transition is sensitive to the ability of the system to transport sand, not simply gravel. To achieve measurable displacement of the GST in natural systems, a significant mass of gravel would need to be transported toward or removed from the toe of the gravel wedge in order to be distinguished from seasonal fluctuations in surficial sand cover that may temporarily cover or uncover underlying gravel.

Some regulated rivers have extensive sand deposits upstream of the historical position of the abrupt GST, giving the impression that mixed gravel-sand bed conditions occur for extended distances upstream of abrupt GSTs. Two well-documented cases are the Rhine and Sacramento rivers, both of which have regulated water discharge and sediment supply. The Sacramento River has sand deposits that extend well upstream of a major break in water surface slope that occurs at the historical position of the GST (Singer, 2008, 2010). The Rhine river has alternating sand and gravel bed reaches over an extended distance (Arbós et al., 2021; Frings, 2011). Observations of sand dunes in gravel reaches of the Rhine River several hundred kilometers upstream of the GST have  $u^*$  values between 0.05 and 0.07 m/s (Carling et al., 2000). Our experiments and the washload deposition theory suggest that anywhere  $u^*$  drops substantially below 0.1 m/s, sand deposits will form upstream of the GST. It would appear that in order for the GST to occur,  $u^*$  must remain  $<0.1$  m/s for an extended reach. The Rhine and Sacramento rivers appear to be natural experiments where flow and sediment supply regulation have caused upstream migration of the GST.

#### 4.4. Synthesis: Controls on GST Formation

Using documented positions of GSTs in global rivers (Dingle et al., 2021) and observations from our experiment, we propose that there are two temporal scales of GST stability. Over  $10^3$ – $10^6$  year timescales, it is generally acknowledged that the position of the GST is controlled by the balance between gravel supply and accommodation (e.g., Paola, Heller, & Angevine, 1992; Paola, Parker, et al., 1992). GSTs are generally found either a short distance downstream of mountain ranges and/or upstream of local or regional base level control that produces a backwater effect on flow. The distance a GST extends into that depositional basin or environment should be a function of the quantity of gravel exported into the basin, and the spatial distribution of accommodation (either vertically through subsidence or sediment compaction, or laterally by channel migration). When averaged over hundred to thousand year time-scales, both gravel supply and the generation of accommodation should be relatively constant, unless responding transiently to a regional tectonic or climatic perturbation (e.g., Blom et al., 2017; Paola, Heller, & Angevine, 1992, Paola, Parker, et al., 1992). Anthropogenic modification of the channel may also result in migration of the stable GST position by increasing or cutting off long-term sediment or water supply (Arbós et al., 2021; Knighton, 1999; Singer, 2010).

We are able to produce stable GSTs in our experiment through both gravel exhaustion and base level change, which creates a transient backwater, and find that the position of the GST can be modified to some degree by changes in  $Q$ ,  $Q_s$ , and  $Q/Q_s$ . The dominant control on the position of the GST is the exhaustion of gravel from the system. In a real system, this would be equivalent to the long-term balance between gravel supply and subsidence, effectively stabilizing the position of the GST. Our results suggest that while  $u^*$  remains above 0.1 m/s, gravel should remain in motion until it is fully exhausted from the supply. Once exhausted, a break in bed gradient should be generated, which causes a reduction in  $u^*$  below 0.1 m/s, forcing sand within the water column to transition from washload to suspended bed material load. Even when the position of the GST should theoretically be stable (i.e., there is no gravel feed or change in base level), observations from our experiments indicate that the point at which  $u^*$  falls below 0.1 m/s can be modified to some degree through shorter-term changes in  $Q$ ,  $Q_s$ , and the sediment delivery ratio  $Q/Q_s$ . We consider this equivalent to seasonal fluctuations in discharge and sediment

supply that can temporarily bury or uncover gravel, and also allow gravel to leak into the diffuse extension of the GST (e.g., Arbós et al., 2021; Venditti et al., 2015, 2019).

## 5. Conclusions

A series of experimental runs documenting changes in sand transport across a stable GST showed that upstream of the GST, sand was transported as washload. Over a distance of ~20–30 cm across the GST, sand rapidly fell out of washload and was transported as suspended bed material load downstream. This change in transport mode created a GST across a narrow range of hydraulic conditions (shear velocity of ~0.10 m/s), which is consistent with the washload theory of Lamb and Venditti (2016). Furthermore, we were able to perturb the position of the GST by changing water and sand supply. Combining our observations, we infer that there are likely two scales of GST stability. While the quantity of gravel and pattern of subsidence downstream of mountain ranges determine the distance at which gravel is exhausted from the system at  $>10^3$  year timescales, seasonal fluctuations in discharge and sand supply drive short-term variability in the position of the GST.

## Data Availability Statement

Details on all experiment parameters and primary data underlying the analysis are presented within the manuscript and are available in full in Zenodo repository <https://doi.org/10.5281/zenodo.6261166> (Dingle & Venditti, 2023).

## Acknowledgments

Experiments, analysis, and writing of this manuscript were supported through an NSERC Discovery Grant and Accelerator Supplement awarded to J.V. The authors are grateful to Kyle Kusack and Morgan Wright for their assistance in building and running the experiments, and to Mike Church for comments on the manuscript. We thank three anonymous reviewers and the Associate Editor for comments which have helped improve the quality of the manuscript.

## References

- Arbós, C. Y., Blom, A., Viparelli, E., Reneerkens, M., Frings, R. M., & Schielen, R. M. J. (2021). River response to anthropogenic modification: Channel steepening and gravel front fading in an incising river. *Geophysical Research Letters*, 48(4), e2020GL091338. <https://doi.org/10.1029/2020GL091338>
- Attal, M., & Lavé, J. (2009). Pebble abrasion during fluvial transport: Experimental results and implications for the evolution of the sediment load along rivers. *Journal of Geophysical Research*, 114(F4), F04023. <https://doi.org/10.1029/2009JF001328>
- Blom, A., Chavarrías, V., Ferguson, R. I., & Viparelli, E. (2017). Advance, retreat, and halt of abrupt gravel-sand transitions in alluvial rivers. *Geophysical Research Letters*, 44(19), 9751–9760. <https://doi.org/10.1002/2017GL074231>
- Bridge, J. S. (2009). *Rivers and floodplains: Forms, processes, and sedimentary record*. John Wiley & Sons.
- Carling, P., Golz, Orr, H. G., & Radecki-Pawlik, A. (2000). The morphodynamics of fluvial sand dunes in the River Rhine, near Mainz, Germany. I. Sedimentology and morphology. *Sedimentology*, 47(1), 227–252. <https://doi.org/10.1046/j.1365-3091.2000.00290.x>
- Church, M. (2006). Bed material transport and the morphology of alluvial river channels. *Annual Review of Earth and Planetary Sciences*, 34(1), 325–354. <https://doi.org/10.1146/annurev.earth.33.092203.122721>
- Church, M., & Hassan, M. (2005). Estimating the transport of bed material at low rate in gravel armoured channels. In R. J. Batalla & C. Garcia (Eds.), *Geomorphological processes and human impacts on river basins* (Publication 299) (pp. 141–153). IAHS.
- Church, M., Hassan, M. A., & Wolcott, J. F. (1998). Stabilizing self-organized structures in gravel-bed stream channels: Field and experimental observations. *Water Resources Research*, 34(11), 3169–3179. <https://doi.org/10.1029/98wr00484>
- Church, M., Wolcott, J. F., & Fletcher, W. K. (1991). A test of equal mobility in fluvial sediment transport: Behavior of the sand fraction. *Water Resources Research*, 27(11), 2941–2951. <https://doi.org/10.1029/91WR01622>
- Colby, B. R. (1963). *Fluvial sediments: A summary of source, transportation, deposition, and measurement of sediment discharge*. U.S. Government Printing Office.
- Cui, Y., & Parker, G. (1998). The arrested gravel front: Stable gravel-sand transitions in rivers Part 2: General numerical solution. *Journal of Hydraulic Research*, 36(2), 159–182. <https://doi.org/10.1080/00221689809498631>
- Curran, J. C., & Wilcock, P. R. (2005). Effect of sand supply on transport rates in a gravel-bed channel. *Journal of Hydraulic Engineering*, 131(11), 961–967. [https://doi.org/10.1061/\(ASCE\)0733-9429\(2005\)131:11\(961\)](https://doi.org/10.1061/(ASCE)0733-9429(2005)131:11(961))
- Dingle, E., & Venditti, J. (2023). Experiments on gravel-sand transitions [Dataset]. Zenodo. <https://doi.org/10.5281/zenodo.6261166>
- Dingle, E. H., Attal, M., & Sinclair, H. D. (2017). Abrasion-set limits on Himalayan gravel flux. *Nature*, 544(7651), 471–474. <https://doi.org/10.1038/nature22039>
- Dingle, E. H., Kusack, K. M., & Venditti, J. G. (2021). The gravel-sand transition and grain size gap in river bed sediments. *Earth-Science Reviews*, 222, 103838. <https://doi.org/10.1016/j.earscirev.2021.103838>
- Dingle, E. H., Sinclair, H. D., Venditti, J. G., Attal, M., Kinnaird, T. C., Creed, M., et al. (2020). Sediment dynamics across gravel-sand transitions: Implications for river stability and floodplain recycling. *Geology*, 48(5), 468–472. <https://doi.org/10.1130/G46909.1>
- Dudill, A., Frey, P., & Church, M. (2017). Infiltration of fine sediment into a coarse mobile bed: A phenomenological study. *Earth Surface Processes and Landforms*, 42(8), 1171–1185. <https://doi.org/10.1002/esp.4080>
- Dudill, A., Venditti, J. G., Church, M., & Frey, P. (2020). Comparing the behaviour of spherical beads and natural grains in bedload mixtures. *Earth Surface Processes and Landforms*, 45(4), 831–840. <https://doi.org/10.1002/esp.4772>
- Einstein, H. A. (1968). Deposition of suspended particles in a gravel bed. *Journal of the Hydraulics Division*, 94(5), 1197–1206. <https://doi.org/10.1061/JYCEAJ.0001868>
- Ferguson, R. (2021). Limits to scale invariance in alluvial rivers. *Earth Surface Processes and Landforms*, 46(1), 173–187. <https://doi.org/10.1002/esp.5006>
- Ferguson, R., Hoey, T., Wathen, S., & Werritty, A. (1996). Field evidence for rapid downstream fining of river gravels through selective transport. *Geology*, 24(2), 179–182. [https://doi.org/10.1130/0091-7613\(1996\)024<0179:FEFRDF>2.3.CO;2](https://doi.org/10.1130/0091-7613(1996)024<0179:FEFRDF>2.3.CO;2)
- Ferguson, R., Hoey, T., Wathen, S., Werritty, A., Hardwick, R., & Smith, G. (1998). Downstream fining of river gravels: Integrated field, laboratory and modeling study. *Gravel-Bed Rivers in the Environment*, 85–114.

- Ferguson, R. I. (2003). Emergence of abrupt gravel to sand transitions along rivers through sorting processes. *Geology*, *31*(2), 159–162. [https://doi.org/10.1130/0091-7613\(2003\)031<0159:EOAGTS>2.0.CO;2](https://doi.org/10.1130/0091-7613(2003)031<0159:EOAGTS>2.0.CO;2)
- Ferguson, R. I., & Church, M. (2004). A simple universal equation for grain settling velocity. *Journal of Sedimentary Research*, *74*(6), 933–937. <https://doi.org/10.1306/051204740933>
- Frey, P. (2014). Particle velocity and concentration profiles in bedload experiments on a steep slope. *Earth Surface Processes and Landforms*, *39*(5), 646–655. <https://doi.org/10.1002/esp.3517>
- Frey, P., Lafaye de Micheaux, H., Bel, C., Maurin, R., Rorsman, K., Martin, T., & Ducotet, C. (2020). Experiments on grain size segregation in bedload transport on a steep slope. *Advances in Water Resources*, *136*, 103478. <https://doi.org/10.1016/j.advwatres.2019.103478>
- Frings, R. M. (2008). Downstream fining in large sand-bed rivers. *Earth-Science Reviews*, *87*(1–2), 39–60. <https://doi.org/10.1016/j.earscirev.2007.10.001>
- Frings, R. M. (2011). Sedimentary characteristics of the gravel–sand transition in the River Rhine. *Journal of Sedimentary Research*, *81*(1), 52–63. <https://doi.org/10.2110/jsr.2011.2>
- Garcia, M. (2008). *Sedimentation engineering*. American Society of Civil Engineers. <https://doi.org/10.1061/9780784408148>
- Graham, D. J., Rice, S. P., & Reid, I. (2005). A transferable method for the automated grain sizing of river gravels. *Water Resources Research*, *41*(7), W07020. <https://doi.org/10.1029/2004WR003868>
- Hassan, M. A., Saletti, M., Johnson, J. P. L., Ferrer-Boix, C., Venditti, J. G., & Church, M. (2020). Experimental insights into the threshold of motion in alluvial channels: Sediment supply and streambed state. *Journal of Geophysical Research: Earth Surface*, *125*(12), e2020JF005736. <https://doi.org/10.1029/2020JF005736>
- Hergault, V., Frey, P., Métivier, F., Barat, C., Ducotet, C., Böhm, T., & Ancey, C. (2010). Image processing for the study of bedload transport of two-size spherical particles in a supercritical flow. *Experiments in Fluids*, *49*(5), 1095–1107. <https://doi.org/10.1007/s00348-010-0856-6>
- Knighton, A. D. (1999). The gravel–sand transition in a disturbed catchment. *Geomorphology*, *27*(3–4), 325–341. [https://doi.org/10.1016/S0169-555X\(98\)00078-6](https://doi.org/10.1016/S0169-555X(98)00078-6)
- Kodama, Y. (1994). Experimental study of abrasion and its role in producing downstream fining in gravel-bed rivers. *Journal of Sedimentary Research*, *64*(1a), 76–85. <https://doi.org/10.2110/jsr.64.76>
- Kuhnle, R. A. (1993). Fluvial transport of sand and gravel mixtures with bimodal size distributions. *Sedimentary Geology*, *85*(1), 17–24. [https://doi.org/10.1016/0037-0738\(93\)90072-D](https://doi.org/10.1016/0037-0738(93)90072-D)
- Lamb, M. P., de Leeuw, J., Fischer, W. W., Moodie, A. J., Venditti, J. G., Nittrouer, J. A., et al. (2020). Mud in rivers transported as flocculated and suspended bed material. *Nature Geoscience*, *13*(8), 566–570. <https://doi.org/10.1038/s41561-020-0602-5>
- Lamb, M. P., & Venditti, J. G. (2016). The grain size gap and abrupt gravel–sand transitions in rivers due to suspension fallout. *Geophysical Research Letters*, *43*(8), 3777–3785. <https://doi.org/10.1002/2016GL068713>
- Lane, E. (1954). *The importance of fluvial morphology in hydraulic engineering (No. Hydraulic Laboratory Report No. 372)*. United States Department of the Interior, Bureau of Reclamation.
- McLean, D. G. (1990). *The relation between channel instability and sediment transport on lower Fraser River*. University of British Columbia. <https://doi.org/10.14288/1.0302167>
- Miller, M. C., McCave, I. N., & Komar, P. D. (1977). Threshold of sediment motion under unidirectional currents. *Sedimentology*, *24*(4), 507–527. <https://doi.org/10.1111/j.1365-3091.1977.tb00136.x>
- Nikora, V., Goring, D., McEwan, I., & Griffiths, G. (2001). Spatially averaged open-channel flow over rough bed. *Journal of Hydraulic Engineering*, *127*(2), 123–133. [https://doi.org/10.1061/\(ASCE\)0733-9429\(2001\)127:2\(123\)](https://doi.org/10.1061/(ASCE)0733-9429(2001)127:2(123))
- Niño, Y., Lopez, F., & Garcia, M. (2003). Threshold for particle entrainment into suspension. *Sedimentology*, *50*(2), 247–263. <https://doi.org/10.1046/j.1365-3091.2003.00551.x>
- Niño, Y., Lopez, F., & Garcia, M. H. (1994). High-speed video analysis of sediment–turbulence interaction. In *Proceedings of the Symposium on Fundamentals and Advancements in Hydraulic Measurements and Experimentation* (pp. 213–222).
- Paola, C. (2001). Modelling stream braiding over a range of scales. In *Gravel-Bed Rivers V* (pp. 11–46). New Zealand Hydrological Society.
- Paola, C., Heller, P. L., & Angevine, C. L. (1992). The large-scale dynamics of grain-size variation in alluvial basins, I: Theory. *Basin Research*, *4*(2), 73–90. <https://doi.org/10.1111/j.1365-2117.1992.tb00145.x>
- Paola, C., Parker, G., Seal, R., Sinha, S. K., Southard, J. B., & Wilcock, P. R. (1992). Downstream fining by selective deposition in a laboratory flume. *Science*, *258*(5089), 1757–1760. <https://doi.org/10.1126/science.258.5089.1757>
- Paola, C., Straub, K., Mohrig, D., & Reinhardt, L. (2009). The “unreasonable effectiveness” of stratigraphic and geomorphic experiments. *Earth-Science Reviews*, *97*(1–4), 1–43. <https://doi.org/10.1016/j.earscirev.2009.05.003>
- Parker, G., & Cui, Y. (1998). The arrested gravel front: Stable gravel–sand transitions in rivers Part I: Simplified analytical solution. *Journal of Hydraulic Research*, *36*(1), 75–100. <https://doi.org/10.1080/00221689809498379>
- Parker, G., Wilcock, P. R., Paola, C., Dietrich, W. E., & Pitlick, J. (2007). Physical basis for quasi-universal relations describing bankfull hydraulic geometry of single-thread gravel bed rivers. *Journal of Geophysical Research*, *112*(F4), F04005. <https://doi.org/10.1029/2006JF000549>
- Roberts, M., & Morningstar, O. (1989). Floodplain formation in a wandering gravelbed river: Lower Fraser River. British Columbia, Canada. *GeoArchaeoRhein*, *2*, 63–70.
- Sambrook Smith, G. H., & Ferguson, R. I. (1995). The gravel–sand transition along river channels. *Journal of Sedimentary Research*, *65*(2), 103838.
- Sambrook Smith, G. H., & Ferguson, R. I. (1996). The gravel–sand transition: Flume study of channel response to reduced slope. *Geomorphology*, *16*(2), 147–159. [https://doi.org/10.1016/0169-555X\(95\)00140-Z](https://doi.org/10.1016/0169-555X(95)00140-Z)
- Seal, R., Paola, C., Parker, G., Southard, J. B., & Wilcock, P. R. (1997). Experiments on downstream fining of gravel: I. Narrow-channel runs. *Journal of Hydraulic Engineering*, *123*(10), 874–884. [https://doi.org/10.1061/\(ASCE\)0733-9429\(1997\)123:10\(874\)](https://doi.org/10.1061/(ASCE)0733-9429(1997)123:10(874))
- Shaw, J., & Kellerhals, R. (1982). *The composition of recent alluvial gravels in Alberta river beds*. Alberta Research Council.
- Singer, M. B. (2008). Downstream patterns of bed material grain size in a large, lowland alluvial river subject to low sediment supply. *Water Resources Research*, *44*(12), W12202. <https://doi.org/10.1029/2008WR007183>
- Singer, M. B. (2010). Transient response in longitudinal grain size to reduced gravel supply in a large river. *Geophysical Research Letters*, *37*(18), L18403. <https://doi.org/10.1029/2010GL044381>
- Toro-Escobar, C. M., Paola, C., Parker, G., Wilcock, P. R., & Southard, J. B. (2000). Experiments on downstream fining of gravel. II: Wide and sandy runs. *Journal of Hydraulic Engineering*, *126*(3), 198–208. [https://doi.org/10.1061/\(ASCE\)0733-9429\(2000\)126:3\(198\)](https://doi.org/10.1061/(ASCE)0733-9429(2000)126:3(198))
- Venditti, J. G., & Church, M. (2014). Morphology and controls on the position of a gravel–sand transition: Fraser River, British Columbia. *Journal of Geophysical Research: Earth Surface*, *119*(9), 1959–1976. <https://doi.org/10.1002/2014JF003147>
- Venditti, J. G., Domarad, N., Church, M., & Rennie, C. D. (2015). The gravel–sand transition: Sediment dynamics in a diffuse extension. *Journal of Geophysical Research: Earth Surface*, *120*(6), 943–963. <https://doi.org/10.1002/2014JF003328>

- Venditti, J. G., Nittrouer, J. A., Allison, M. A., Humphries, R. P., & Church, M. (2019). Supply-limited bedform patterns and scaling downstream of a gravel–sand transition. *Sedimentology*, *66*(6), 2538–2556. <https://doi.org/10.1111/sed.12604>
- Wathen, S. J., Ferguson, R. I., Hoey, T. B., & Werritty, A. (1995). Unequal mobility of gravel and sand in weakly bimodal river sediments. *Water Resources Research*, *31*(8), 2087–2096. <https://doi.org/10.1029/95WR01229>
- Wilcock, P. R. (1998). Two-fraction model of initial sediment motion in gravel-bed rivers. *Science*, *280*(5362), 410–412. <https://doi.org/10.1126/science.280.5362.410>
- Wilcock, P. R., & Crowe, J. C. (2003). Surface-based transport model for mixed-size sediment. *Journal of Hydraulic Engineering*, *129*(2), 120–128. [https://doi.org/10.1061/\(ASCE\)0733-9429\(2003\)129:2\(120\)](https://doi.org/10.1061/(ASCE)0733-9429(2003)129:2(120))
- Wilcock, P. R., & Kenworthy, S. T. (2002). A two-fraction model for the transport of sand/gravel mixtures. *Water Resources Research*, *38*(10), 12-1–12-12. <https://doi.org/10.1029/2001WR000684>
- Wilcock, P. R., Kenworthy, S. T., & Crowe, J. C. (2001). Experimental study of the transport of mixed sand and gravel. *Water Resources Research*, *37*(12), 3349–3358. <https://doi.org/10.1029/2001WR000683>
- Williams, G. P. (1970). *Flume width and water depth effects in sediment-transport experiments*. U.S. Government Printing Office.
- Wolcott, J. (1988). Nonfluvial control of bimodal grain-size distributions in river-bed gravels. *Journal of Sedimentary Research*, *58*(6), 979–984. <https://doi.org/10.1306/212F8ED6-2B24-11D7-8648000102C1865D>
- Yalin, M. S., & Karahan, E. (1979). Inception of sediment transport. *Journal of the Hydraulics Division*, *105*(11), 1433–1443. <https://doi.org/10.1061/JYCEAJ.0005306>
- Yatsu, E. (1955). On the longitudinal profile of the graded river. *Eos, Transactions American Geophysical Union*, *36*(4), 655–663. <https://doi.org/10.1029/TR036i004p00655>